Accepted Manuscript

Grain-size distribution of volcaniclastic rocks 2: Characterizing grain size and hydraulic sorting

Martin Jutzeler, Jocelyn McPhie, Sharon R. Allen, A.A. Proussevitch

Please cite this article as: Jutzeler, Martin, McPhie, Jocelyn, Allen, Sharon R., Proussevitch, A.A., Grain-size distribution of volcaniclastic rocks 2: Characterizing grain size and hydraulic sorting, *Journal of Volcanology and Geothermal Research* (2015), doi: 10.1016/j.jvolgeores.2015.05.019
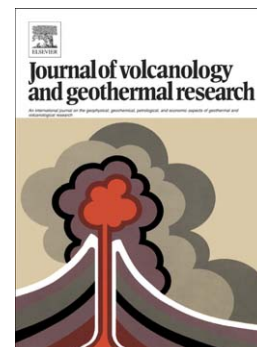
Grain-size distribution of volcaniclastic rocks 2: Characterizing grain size and hydraulic sorting

Martin Jutzeler[1][*], Jocelyn McPhie[1], Sharon R. Allen[1], Proussevitch A.A.[2],

1: CODES – ARC Centre of Excellence in Ore Deposits, University of Tasmania, PO Box 79, Hobart 7005, Australia
2: Earth Systems Research Center, Institute for the Study of Earth, Oceans, and Space, University of New Hampshire, Durham, NH 03824, United States of America

First author's current contact address:
Dr. Martin Jutzeler
National Oceanography Centre, Southampton
European Way, Waterfront Campus
Southampton, SO14 3ZH
United Kingdom
jutzeler@gmail.com
+44 23 80596 559

Highlights:

Functional stereology is efficient to interpret sedimentation mechanisms

Simple hydraulic sorting ratios allow inference on styles of deposition

Transport and deposition mechanisms can be evaluated from pumiceous rocks

Modes are more adequate than median to characterize sediment grain size

Abstract

Quantification of the grain size distribution of sediments allows interpretation of processes of transport and deposition. Jutzeler et al. (2012) developed a technique to determine grain size distribution of consolidated clastic rocks using functional stereology, allowing direct comparison between unconsolidated sediments and rocks. Here, we develop this technique to characterize hydraulic sorting and infer transport and deposition processes. We compare computed grain size and sorting of volcaniclastic rocks with field-based characteristics of volcaniclastic facies for which transport and depositional mechanisms have been inferred. We studied pumice-rich, subaqueous facies of volcaniclastic rocks from the Oligocene Ohanapecosh Formation (Ancestral Cascades, Washington, USA), Pliocene Dogashima Formation (Izu Peninsula, Honshu, Japan), Miocene Manukau Subgroup (Northland, New Zealand) and the Quaternary Sierra La Primavera caldera (Jalisco State, Mexico). These sequences differ in bed thickness, grading and abundance of matrix. We propose to evaluate grain size and sorting of volcaniclastic deposits by values of their modes, matrix proportion (<2 mm; F-1) and D_{16}, instead of median diameter (D_{50}) and standard deviation parameters. F-1 and D_{16} can be uniformly used to characterize and compare sieving and functional stereology data. Volcaniclastic deposits typically consist of mixtures of particles that vary greatly in density and porosity. Hydraulic sorting ratios can be used to test whether inferred density of mixed clast populations of pumice and dense clasts are hydraulically sorted with each other, considering various types of transport under water. Evaluation of this ratio for our samples shows that most studied volcaniclastic facies are deposited by settling from density currents, and that basal dense clast breccia are emplaced by shear rolling. These hydraulic

sorting ratios can be applied to any type of clastic rocks, and indifferently on consolidated and unconsolidated samples.

1. Introduction

The interpretation of mechanisms of transport and deposition for detrital sediments has been in use for at least five decades, and relies on field characteristics, grain size and sorting (Friedman, 1962; Kuno et al., 1964; Passega, 1964; Visher, 1969; Buller and McManus, 1973; Glaister and Nelson, 1974; Garzanti et al., 2009). In addition, variations in grain size distribution, sorting and componentry of pyroclastic deposits with distance from source are important attributes used to constrain models of subaerial explosive eruptions and volcaniclastic density currents (e.g. Walker, 1971; Sparks et al., 1973; Sparks, 1976; Walker, 1983, 1984; Wilson and Walker, 1985; Carey, 1991; Bonadonna and Houghton, 2005; Dufek and Bergantz, 2007; Macedonio et al., 2008; Volentik et al., 2010; Alfano et al., 2011; Mackaman-Lofland et al., 2014). Sorting and grading are two critical values from which inferences can be made on processes of transport and deposition.

Furthermore, these grain-size based physical models of transport and deposition have not been applied to lithified and/or welded deposits, although these rocks are far more abundant on Earth than unconsolidated deposits. We apply the image analysis and functional stereology technique using predefined distribution functions (Proussevitch et al., 2007a; Proussevitch et al., 2007b) adapted for (consolidated) clastic rocks (Jutzeler et al., 2012) for assessing the grain size characteristics of subaqueous volcaniclastic facies, which are mostly lithified and commonly contain less fines than their subaerial analogues. In this paper, we refer to this technique as functional stereology as it implicitly combines statistical functions with earlier formulations of

stereological transformations (Sahagian and Proussevitch, 1998). The grain size distribution of the samples studied in this paper were calculated as following a log-normal behavior, as does a large selection of natural object sizing categories (Proussevitch et al., 2007a; Proussevitch et al., 2007b). Following formulations from our previous work (Jutzeler et al., 2012), we use normal (Gaussian) continuous distribution for clast sizes in phi (ϕ) units (Krumbein, 1936) as the predefined function, equivalent to log-normal distribution with respect to linear units (e.g. meters). Assumed conformity of 2D (cross-section areas) and 3D (volumes) distribution functions will be researched in our future studies.

Previous work on use of grain size distribution to infer depositional processes include Visher (1969) and Glaister and Nelson (1974), who proposed a classification of multi-modal distributions based on the segmentation pattern of cumulative curves and histograms of grain size distribution on unconsolidated deposits. Their method was designed to discriminate among three major types of transport (traction, saltation, suspension), but could be applied only to certain types of detrital sediments (Sengupta et al., 1991), and has not been tested on volcaniclastic deposits. Wohletz et al. (1989) proposed the sequential fragmentation/transport model, which deconvolutes grain size distribution curves into sub-population modes, allowing inference on complex fragmentation and transport histories.

The median and standard deviation of grain diameters in unconsolidated deposits are the parameters most widely used to infer transport and depositional processes for volcaniclastic deposits (Murai, 1961; Walker, 1971, 1983, 1984). Some of these parameters can be directly applied to clastic rocks, but fine components are, in most cases, not resolvable. There is a major issue in comparing median values, as they are dependent on the studied range, and are commonly wrongly applied to multimodal

distributions (Folk, 1980). We find the use of mode and D_{16} (Inman, 1952) as more meaningful parameters, and introduce F-1, the ratio of matrix (anything <2 mm).

The mechanisms of transport for subaqueous volcaniclastic density currents are poorly understood in comparison to their siliciclastic homologues (Manville et al., 1998; White, 2000; Manville et al., 2002; Freundt, 2003; Manville and Wilson, 2004; Allen and Freundt, 2006; Talling et al., 2012), as they commonly contain coarse clasts of varying density (pumice or scoria), which are much less dense than conventional dense (i.e. non to poorly-vesicular) clasts. Hydraulic sorting refers to sorting of clasts during transport in a fluid with non-negligible drag. The terminal velocity of a clast in motion in a fluid is dependent of the viscosity and density of the fluid, and of the size, bulk density and shape of the clast (e.g. Rubey, 1933; Clift et al., 1978; Komar and Reimers, 1978; Sallenger, 1979; Komar et al., 1984; Cashman and Fiske, 1991; Kano, 1996; Crowe et al., 1998; Manville and Wilson, 2004; Dellino et al., 2005; Burgisser and Gardner, 2006). Hydraulic equivalence refers to the condition where clasts differing in size and density are deposited similarly (Burgisser and Gardner, 2006).

In this paper, the grain size distribution of coarse (>2 mm) fraction of volcaniclastic rocks deposited under water is statistically reconstructed by image analysis and functional stereology, using photographs of outcrops and scans of rock slabs (Jutzeler, 2012; Jutzeler et al., 2012). We explore grain size characteristics in terms of modal grain size distribution, matrix ratio, and statistical parameters such as median (D_{50}), D_{16}, and standard deviation. We propose the degree of hydraulic sorting of pumice with dense clasts to infer the original pumice vesicularity and test field-based interpretations of the main transport and depositional processes under water, including fall, saltation, and various types of rolling, adapting the equations of Burgisser and Gardner (2006) to underwater conditions. This research is novel in using simple ratios

to evaluate the subaqueous transport processes for consolidated or unconsolidated deposits composed of clasts with variable density. Our method can be applied to any clastic rock or sediment, using grain size data from various methods (e.g. sieving, laser diffraction, functional stereology), thus widely applicable in sedimentology and volcanology-oriented studies.

1.1. Rock suites

Image analysis and functional stereology were performed on a statistically significant sample suite comprising 85 volcaniclastic samples selected from different origins and from several localities. Most samples belong to the Pliocene Dogashima (Izu Peninsula, Japan) and Oligocene Ohanapecosh (Ancestral Cascades, USA) formations (Fiske, 1963; Cashman and Fiske, 1991; Jutzeler, 2012; Jutzeler et al., 2014a; Jutzeler et al., 2014b). Additional samples were collected in the Miocene Manukau Subgroup (Northland, New Zealand; Allen et al., 2007; Jutzeler, 2012) and in the Quaternary Sierra la Primavera caldera (Jalisco State, Mexico; Clough et al., 1981). The computed grain size data are based on 165 images and are combination of up to three size-nested datasets from outcrop photographs and rock slab scans taken at different magnifications (Jutzeler et al., 2012). Size-nesting in coarse (>2 mm) clast distributions is simpler than for µm-to-mm-sized vesicles in pyroclasts (e.g. Shea et al., 2010), because coarse clasts are commonly relatively homogeneously distributed, and their shape is relatively equant. In addition, we do not consider fine grains in this study. However, high-precision image analysis is complex, as clasts touch others, and clast types, fabric, and color vary substantially among samples.

1.2. Clast componentry

Clastic rocks may contain one or multiple types of clasts (>2 mm), matrix, interstitial pore space and cement. The clast types in the samples analyzed are grouped into two

categories for simplicity: 1) Pumice clasts, which contain ~60–90 vol.% vesicles; some have been compacted to form fiamme. "Deflattening" of the fiamme (Jutzeler et al., 2012) could not be carried out in these examples because the fiamme and pumice clasts coexist in some facies and the original pumice clast vesicularity is unknown. Fiamme only occur in some beds of the Ohanapecosh Formation and are assumed to not substantially modify these data. The density of waterlogged pumice clasts is assumed to range between 1,100 and 1,600 kg/m^3, corresponding to 60–95 vol.% vesicularity of a waterlogged clast with density of 2,500 kg/m^3 at dense rock equivalent. 2) Dense (non-vesicular) clasts and hydrothermally altered clasts; densities for these clasts is assumed to have been 2,500 kg/m^3, corresponding to rocks of intermediate composition.

1.3. Matrix cut-off

The original texture of fine grained particles, typically <2 (>-1 ϕ) in clastic rocks, is commonly destroyed or poorly preserved, or difficult to resolve. In eruption-fed volcaniclastic facies, sub-mm clasts generally have the same composition in the coarse clasts, and are likely to be a continuation of the coarse modal clast populations. Two millimeters is a critical boundary that separates sand from gravel, sandstone from breccia or conglomerate, ash from lapilli, and tuff from pyroclastic breccia in clastic deposits (Wentworth, 1922; McPhie et al., 1993; Blott and Pye, 2001; White and Houghton, 2006), thus 2 mm is used in this study to distinguish between clasts and matrix. Hereafter, we keep loose definition for grains and particles, which can be fine (<2 mm) or coarse (>2 mm). For simplicity all particles <2 mm, filling or void are called matrix in this study even though cement and porosity might also be present. Cement is a post-depositional, chemical and/or biochemical precipitate that may partly or completely fill the porosity left between particles that constitute the sediment

(matrix and/or clasts). In a rare case (Manukau Subgroup), cement could be separated from matrix, and this sample is clearly identified (Fig. 1).

2. Quantification of textural characteristics in volcaniclastic beds

2.1. Clast volume

Stratigraphic logs are commonly based on visual estimates in the field, and reproduce the main textural characteristics including approximate mean and maximum grain size. The image analysis method (Jutzeler et al., 2012) quantifies clast and matrix volumes (Figs 1, 2). Data extracted from image analysis give a large choice of parameters on which to characterize and classify clastic aggregates. One of the most straightforward parameters is determining the volume of components, as volume is directly proportional to its area on a representative cross section (Reid, 1955), in contrast to object size distribution (Proussevitch et al., 2007b; Jutzeler et al., 2012). Volumes of components in clastic rocks can therefore be determined as:

$$V_{Tot} \cong A_{Matrix} + A_{Pum} + A_{Dense} \tag{1}$$

where V_{Tot} is the total volume of the sample, A_{Matrix} is the total area of grains <2 mm (and includes cement and porosity), and A_{Pum} and A_{Dense} are the areas of pumice and dense clasts coarser than 2 mm, respectively. Using poorly consolidated sediments, such calculation is only valid where using a representative, non-eroded outcrop in which large clasts are not preferentially hanging out of the cliff face at the expense of poorly consolidated matrix (Jutzeler et al., 2012). The comparison of volume of coarse clasts with fine clasts and cement in a deposit can be used as proxy for the degree of sorting. Sorting is inversely proportional to the degree of packing of clasts (Jerram et al., 1996). We introduce the parameter F-1, which is the percentage of clasts <2 mm (or >-1 ϕ) and/or void or cement in a deposit.

2.2. Grain size distribution

The output from functional stereology code gives the grain size distribution density (G_i) in $(m^3\phi)^{-1}$, calculated as average clast diameters in each size class (bin *i*). From G_i, the volume of clasts in $(m^3\phi)^{-1}$ (V_i) can be calculated (Jutzeler et al., 2012). Modal values of volume V_i of pumice and dense clasts can be extracted from modal grain size distribution densities G_i (Figs 1d, 1e, 2d, 2e). The modal distribution of V_i represents the statistically most likely abundant grain sizes, thus this it is a meaningful measurement of the physical property (grain size) of the clastic rock. Moreover, it corresponds to the commonly estimated values of grain size in field and laboratory descriptions. Here, only modal V_i is discussed, because it is easier to represent and compare volumes than distribution densities.

Image stereology computes V_i, which can be converted to weight percent, by adjusting V_i to the density of each clast type (Jutzeler et al., 2012). To simplify the conversion, the densities of pumice clasts versus dense clasts are taken to be homogeneous. Here, we use a density of 2,500 kg/m^3 (0% vesicles) for dense clasts and 700 kg/m^3 (72% vesicles) for air-filled pumice clasts, corresponding to common volcanic rock densities. Total clast weight percent is a combination of weight percent datasets for pumice and dense clasts which is then recalculated to 100% (Jutzeler et al., 2012).

Significant values such as modes, D_{16}, D_{50} (i.e. median, M_ϕ), D_{84}, and standard deviation σ_ϕ (i.e. sorting) were extracted from G_i, V_i and weight percent distributions with *Gradistat* (Blott and Pye, 2001), using the graphical measures of Folk and Ward (1957). Graphical measures are preferred to values from methods of moments, which give too much importance to the tails of the distribution (Folk, 1980), although both measures give very similar values using our dataset.

The median diameter M_ϕ and standard deviation σ_ϕ of grain size distributions reflect the average grain size and degree of grain size sorting, respectively. Both median diameter and standard deviation are commonly computed for unconsolidated subaerial pyroclastic deposits and the data plot in fields relating to transport and depositional processes (Murai, 1961; Walker, 1971, 1983, 1984). However, such data should be used with extreme caution, because several conditions are needed to correctly calculate, correlate and interpret such data (see Discussion). As this study uses statistical measurements applied for particles >2 mm only, calculations using functional stereology shifts the median and standard deviation to overall lower values, which means samples appear to be coarser and better sorted than they are (Figs 1g, 2g). Hence, such data remains informative only, and cannot be directly compared with conventional data that includes fine particles (e.g. Walker, 1983).

2.3. Hydraulic equivalence and hydraulic sorting

2.3.1 Hydraulic equivalence in subaqueous volcaniclastic deposits

Hydraulic equivalence is the condition where particles of different size and density have similar terminal velocity during their sedimentation in a continuous fluid (Rubey, 1933; Clift et al., 1978; Cashman and Fiske, 1991; Kano, 1996; Manville et al., 2002; Burgisser and Gardner, 2006). The hydrodynamic properties of natural particles depend on multiple factors related to the particle, such as density, size, shape (~aspect ratio), surface roughness, as well as the type of ambient fluid (air, dusty gas, steam or seawater) and interactions with other particles (Manville et al., 2002; Manville and Wilson, 2004; Burgisser and Gardner, 2006; Alfano et al., 2011). Hydraulic sorting may be achieved in various conditions of sedimentation, where these hydrodynamic properties may be variably preponderant (Burgisser and Gardner, 2006). For instance, a large and low-density pumice clast falling in a fluid will have

similar terminal velocity to a smaller but denser clast, however hydraulic sorting during shear rolling is chiefly not dependent of the density of both clast and ambient fluid (see below; Burgisser and Gardner, 2006). Although the grain size distribution of a clastic deposit reflects the diameters of clasts, it does not give much information on the circumstances of clast deposition. Instead, hydraulic sorting reflects whether or not constituents of a clastic aggregate were deposited together under hydraulic equivalence, and under which style of transport. This is a much better approach to understand the natural conditions of sedimentation. One way to produce hydraulically well sorted natural deposits is by the vertical fall of discrete grains at their terminal velocity (suspension settling). The type of fluid, with its specific viscosity, has great importance. The degree of waterlogging is defined by the relative volume of liquid water versus gas in the pore spaces of a pumice clast. From the equations of Clift et al. (1978), Cashman and Fiske (1991) proposed a hydraulic equivalence ratio of 5–10 to 1 for the diameters of waterlogged pumice clasts (1,100-1,300 kg/m^3) versus coarse dense clasts (2,500 kg/m^3) during free fall in seawater. In contrast, a ratio of 2–3 to 1 characterizes grain diameters of coarse pumice clasts versus dense clasts in free fall in air. This difference indicates that, in this case, water is a better "sorting agent" than air (e.g. Cashman and Fiske, 1991; Manville et al., 2002), because of its higher density. The range in these ratios reflects variation in clast densities, in particular the vesicularity and degree of waterlogging of the pumice clasts, as well as discrepancies from grain shape (Clift et al., 1978; Komar and Reimers, 1978; Cashman and Fiske, 1991; Alfano et al., 2011). In addition, where fine particles are in large concentrations, vertical density currents may form and travel 1 to

3 orders of magnitude faster than discrete particles settling from suspension (Wiesner et al., 1995; Carey, 1997; Manville and Wilson, 2004).

In this paper, we follow the equation for terminal velocity (U_T) as presented in Burgisser and Gardner (2006):

$$U_T = \frac{4\Delta\rho d^2 g}{3\mu C_D \, \text{Re}} \tag{2}$$

where $\Delta\rho$ in kg/m^3 is the difference between the particle density (ρ_i) and the fluid density (ρ_f), with $\Delta\rho = (\rho_i - \rho_f)$ to account for Archimedes' force, g is the acceleration due to gravity (m/s^2), d is the particle diameter (m), μ is the water viscosity (Pa·s), C_D is the drag coefficient and Re is the dimensionless Reynolds number. Substituting:

$$\text{Re} = \frac{\rho_f U_T d}{\mu} \tag{3}$$

we obtain:

$$U_T = \sqrt{\frac{4\Delta\rho dg}{3C_D\rho_f}} \tag{4}$$

This equation is appropriate for high Reynolds numbers, where $C_D \approx 0.45$ (Clift et al., 1978; Crowe et al., 1998; Burgisser and Gardner, 2006). Sedimentation of clasts (>2 mm) in water chiefly correspond to the range $750 < Re < 3.5 \times 10^3$. From the above equation, assuming g/C_D constant, particles with the same ratio of:

$$\left(\frac{\rho_i - \rho_f}{\rho_f}\right)d_i \tag{5}$$

have the same U_T or are 'hydraulically equivalent'.

Styles of sedimentation in subaerial setting including settling from: a suspended-load during progressive aggradation, discrete vertical fallout, saltation, and saltation and packed rolling, can be approximated (Burgisser and Gardner, 2006) by:

$$\rho_{Dense}d_{Dense} \cong \rho_{Pum}d_{Pum} \qquad\qquad \text{, for Re} > 10^3 \quad (6)$$

In contrast to gaseous environments, seawater density is not negligible. To estimate the hydraulic sorting by settling in water, we modify equation (6) into:

$$\left(\frac{\rho_{Dense} - \rho_{fluid}}{\rho_{fluid}}\right)d_{Dense} \cong \left(\frac{\rho_{Pum} - \rho_{fluid}}{\rho_{fluid}}\right)d_{Pum} \qquad \text{, for Re} > 10^3 \quad (7)$$

where ρ_{Dense} is the density of dense clasts ($\sim$2,500 kg/m^3), ρ_{Pum} is the density of waterlogged pumice clasts ($\sim$1,100–1,500 kg/m^3, which corresponds to 68–95 vol.% vesicles), ρ_{fluid} is the ambient fluid density (seawater; 1,025 kg/m^3) and d_{Pum} and d_{Dense} are the diameters of pumice clasts and dense clasts, respectively.

For deposition by collision-induced rolling, Burgisser and Gardner (2006) proposed:

$$\rho_{Dense}d_{Dense}^4 \cong \rho_{Pum}d_{Pum}^4 \qquad\qquad \text{, for Re} > 10^3 \quad (8)$$

In underwater conditions, a similar modification needs to be applied than for equation (7), with:

$$\left(\frac{\rho_{Dense} - \rho_{fluid}}{\rho_{fluid}}\right)d_{Dense}^4 \cong \left(\frac{\rho_{Pum} - \rho_{fluid}}{\rho_{fluid}}\right)d_{Pum}^4 \qquad \text{, for Re} > 10^3 \quad (9)$$

Under deposition by shear rolling conditions, clast density becomes negligible, and clasts are chiefly sorted by their size, giving (Burgisser and Gardner, 2006):

$$d_{Dense} \cong d_{Pum} \qquad\qquad \text{, for Re} > 10^3 \quad (10)$$

, which is applicable to underwater conditions with no modification.

Equations (6–10) are valid only for relatively high Reynolds numbers (Re$>10^3$) that correspond, at terminal velocity, to waterlogged pumice clasts larger than 5–8 mm (depending on their vesicularity) and dense clasts larger than 3 mm. This minimum grain size is compatible within most ranges of grain size populations studied here. The bulk density of pumice clasts depends on the volume, type, and density of the fluid that fills the vesicles (Manville et al., 1998; White et al., 2001; Manville et al., 2002).

The pumice clasts are considered to have been cold and entirely waterlogged, thus to contain no gas (air, magmatic gas). This assumption is reasonable, considering that hot pumice clasts are quickly waterlogged when put in contact with water (Whitham and Sparks, 1986; Allen et al., 2008), that >90 vol.% of the vesicles are connected in most pumice clasts (Klug et al., 2002), and that the increasing hydrostatic pressure with transport to deeper water results in the contraction and resorption of any remaining gas in the vesicle network.

2.3.2. Hydraulic sorting ratios in subaqueous volcaniclastic deposits

Hydraulic sorting can be determined within a graded facies, or between facies of subaqueous volcaniclastic deposits. Here, we propose a simple set of equations to assess the hydraulic sorting of clastic aggregate containing clast populations that have different bulk densities (e.g. pumice versus dense clasts). We propose the term of hydraulic sorting ratio for the parameter that indicates whether the grain sizes of pumice and dense clasts in natural samples are consistent with them being hydraulically equivalent, and apply the three types of conditions of sedimentation previously described, each of them having a specific hydraulic sorting ratio. Following equations (7), (9), and (10), respectively, we define three hydraulic sorting ratios (HSR), with:

$$HSR_{settling} = \left(\frac{\rho_{Pum} - \rho_{Fluid}}{\rho_{Pum}} \right) d_{Pum} \bigg/ \left(\frac{\rho_{Dense} - \rho_{Fluid}}{\rho_{Dense}} \right) d_{Dense} \quad , \text{for Re} > 10^3 \quad (11)$$

, for sedimentation from settling from: suspended-load during progressive aggradation, discrete vertical fallout, saltation, and saltation and packed rolling.

For sedimentation by collision-induced rolling, we propose:

$$HSR_{coll-roll} = \left(\frac{\rho_{Pum} - \rho_{Fluid}}{\rho_{Pum}} \right) d_{Pum}^4 \bigg/ \left(\frac{\rho_{Dense} - \rho_{Fluid}}{\rho_{Dense}} \right) d_{Dense}^4 \quad , \text{for Re} > 10^3 \quad (12)$$

Finally, for shear rolling, we propose:

$$HSR_{shear-roll} = d_{Pum}/d_{Dense} \qquad\qquad \text{, for Re} > 10^3 \quad (13)$$

A deposit is hydraulically sorted if the hydraulic sorting ratio equals 1. Values higher than 1 indicate that the pumice clasts are too coarse to be hydraulically equivalent to dense clasts in the same sample. Conversely, values lower than 1 imply that the pumice clasts are too small to be in hydraulic equivalence with the dense clasts. These parameters have the advantages over traditional grain size sorting data, from sieving and laser diffraction, of being related to the environment and style of deposition and to take the particle vesicularity into account, and of not being exclusively related to the diameter of the particles and average bulk densities. This calculation should give similar results to measurements using settling tubes or wave tanks, although our technique also analyses the componentry ratio and grain size distribution of each clast population, and allows inference of their wet density.

The clast diameters d_{Pum} and d_{Dense} are best approximated by the value of the primary modes. The value of the main mode is preferred to the median, because the mode reflects the most abundant clast size, whereas the median is strongly dependent on the matrix minimum cut-off size and is less representative of the coarse clast population. The hydraulic sorting ratio of the secondary modes can be assessed in the same way, although the evaluation of hydraulic sorting between secondary modes becomes increasingly complex for multimodal populations. Because the original pumice clast vesicularity and degree of waterlogging may be difficult to assess, a range of densities are tested for graded deposits (Figs 1, 2): at one extreme, waterlogged pumice clasts at 1,100 kg/m^3 (very highly vesicular (95%), corresponds to 130 kg/m^3 when dry) and 1,500 kg/m^3 (highly vesicular (68%), corresponds to 800 kg/m^3 when dry). Dense (non-vesicular) clasts density is fixed at 2,500 kg/m^3.

3. Application to field-based examples

Results of facies analysis (Jutzeler, 2012; Jutzeler et al., 2014a; Jutzeler et al., 2014b) are used to test whether proportional volume and grain size distribution of coarse (>2 mm) clasts in graded volcaniclastic beds indicate specific types of transport and depositional processes in a context of submarine volcanism. In particular, we analyze the most likely subaqueous transport mechanisms using the hydraulic equivalence signature in context of deposition from vertical settling, collision-induced rolling and shear rolling, through stratigraphy of thick, graded deposits.

3.1. Subaqueous volcaniclastic facies

The studied samples are chiefly composed of pumice clasts, and their content of fine clasts is variable; a large proportion of our samples are dominated by matrix (>50 vol.%) and poor in dense clasts (<20 vol.%). From the dataset available, three broad subaqueous volcaniclastic facies could be identified on the basis of bed thickness, degree of sorting and matrix ratio. These facies include (Table 1) two very thick, graded facies that can be divided into matrix-rich (>50 vol.%; MR-thick) and matrix-poor (<50 vol.%; MP-thick) types. The third facies is a thin to thick (<1 m), clast-supported, well sorted and matrix-poor facies (MP-thin). The matrix ratio is used to discriminate between facies MR-thick and MP-thick, because the abundance of fine-grained particles may be a good indicator of transport and depositional processes (Walker, 1971; White, 2000; Jutzeler, 2012; Talling et al., 2012), and is simple to assess from image analysis. The matrix-rich, very thick, graded facies (MR-thick) have overall the highest abundance of dense clasts, and commonly contains a basal dense-clast breccia sub-facies that is depleted in matrix (e.g. bed Cayuse 40; Fig. 2).

Graded beds are difficult to classify, because textural characteristics such as grain size, componentry and volume of matrix vary through the stratigraphy (Figs 1, 2). For the gradational facies, the matrix proportion is taken as the average over the deposit thickness. Thus, several samples of matrix-poor, very thick, graded facies (MP-thick) have an overall matrix-rich signature (Figs 1, 2), because they are the fine-grained sub-facies (generally the upper part of a normally graded bed) of overall matrix-poor beds (Fig. 1). Conversely, an overall matrix-rich, graded deposit that contains a minor basal, matrix-poor, clast-supported sub-facies is regarded as an overall matrix-rich facies.

3.1.1. Matrix-rich, very thick, graded facies

The matrix-rich, very thick, graded facies (MR-thick) includes examples from the Ohanapecosh Formation, the Dogashima Formation, and the Manukau Subgroup (Jutzeler, 2012; Jutzeler et al., 2014a; Jutzeler et al., 2014b). Typical examples comprise graded beds 57 and 61 in the Chinook Pass section, beds 40 and 42 in the Cayuse Pass section (Chinook Pass Member), and bed B-3 at Cougar Lake (Jutzeler et al., 2014b). These five beds in the Ohanapecosh Formation were interpreted as deposits from eruption-fed and resedimented subaqueous volcaniclastic density currents, and most likely to be related to subaerial, pumice-rich pyroclastic flows that entered water.

3.1.2. Matrix-poor, very thick, graded facies

The matrix-poor, very thick, graded facies (MP-thick) occur in the Dogashima Formation and the Ohanapecosh Formation (Jutzeler et al., 2014a; Jutzeler et al., 2014b). The most typical example is the bed of grey andesite breccia (D2-2) overlain by white pumice breccia (D2-3) in Dogashima 2 (Jutzeler et al., 2014a). These two clast-supported facies were interpreted to have been simultaneously deposited from a

pumice-rich, subaqueous volcaniclastic density current derived from destruction of a subaqueous, hot, dense lava dome by a pumice-forming, explosive eruption (Tamura et al., 1991; Jutzeler et al., 2014a).

3.1.3. Matrix-poor, thin to thick, clast-supported, well sorted facies

The matrix-poor, thin to thick, clast-supported, well sorted facies (MP-thin) were sampled in the Manukau Subgroup, the Ohanapecosh Formation, the Dogashima Formation and the Primavera caldera (Jutzeler, 2012; Jutzeler et al., 2014a; Jutzeler et al., 2014b). This facies is exemplified by normally graded pumice-rich beds at Bethells Beach and Pillow Lava Bay in the Manukau Subgroup, New Zealand (Allen et al., 2007; Jutzeler, 2012), interpreted as deposited from subaqueous vertical settling through the water column. Although they are very thickly bedded, the samples from Sierra La Primavera caldera, interpreted as suspension settled giant pumice clasts (Clough et al., 1981), are also included in this third facies, because the interpreted transport process involved discrete settling of the pumice clasts in a confined environment (caldera lake) producing an abnormally thick and coarse deposit.

3.1.4. Examples of graded beds

Figures 1 and 2 show examples of outputs for graded beds in the Ohanapecosh Formation, the Dogashima Formation and the Manukau Subgroup. The modal grain size distribution density G_i and volume V_i show variations in grain size in the stratigraphy and consistently follows field estimates summarized as logs. Coarse clasts are generally bimodally distributed. The volume distribution within the fiamme-bearing Ohanapecosh Formation includes uncertainties because of the unknown original porosity of the compacted pumice clasts. Hence, modal diameter of these compacted pumice clasts may generate smaller average diameter than the original clast size (Jutzeler et al., 2012).

3.2. Median diameter and sorting

The grain size distributions of various types of subaqueous volcaniclastic deposits overlap on the standard deviation versus median plot (Fig. 3). The extreme coarseness of pumice clasts (>5 m) in matrix-poor, thin to thick, clast-supported, well sorted facies (MP-thin) in the Sierra La Primavera caldera gives extreme median values of ~-9.5 ϕ. Examples of this facies do not show standard deviation values higher than 1.2, whereas this parameter reaches 1.6 in both of the very thick facies.

We compare the value of standard deviation versus median from functional stereology of volcaniclastic rocks with data from sieving of subaerial unconsolidated pyroclastic deposits (Fig. 4). The exclusion of the matrix data in this study (weight percent data ranges -12 to -1 ϕ) results in a bias to relatively coarse and well-sorted values (Fig. 4a–d), compared to data on unconsolidated grain size populations determined by Walker (1983), who sieved pyroclastic deposits between -5 to 5 ϕ. The subaqueous volcaniclastic rocks dataset overlaps with subaerial plinian fall and fines-depleted pyroclastic flow fields of Walker (1983), which indicates good sorting and relatively coarse populations. Because the original raw data from Walker (1983) are unpublished, we use the sieving data of the ignimbrite units D and E of the Kos Plateau Tuff (KPT; Allen et al., 1999) as an approximation of pyroclastic flow deposits. This estimation is justified considering the total weight percent data (-4 to +5 ϕ) of KPT ignimbrites fit in the coarse and well-sorted end of the pyroclastic flow field (Fig. 4b) in the standard deviation versus median plot of Walker (1983). KPT ignimbrite (sieving) and subaqueous volcaniclastic (functional stereology) data match each other when using the same cut-off in grain size (>2 mm). Particularly, the coarse-grained KPT ignimbrite data match the functional stereology field for matrix-rich, very thick, graded facies (MR-thick; Fig. 4b).

The overlap between coarse-grained weight-percent data of KPT subaerial ignimbrite and matrix-rich, very thick, graded facies (MR-thick) gives additional confirmation that functional stereology data match results from the sieving technique (Jutzeler et al., 2012). There is a large overlap between median and standard deviation of coarse clasts in the three subaqueous volcaniclastic facies. Using coarse clasts only, it is difficult to distinguish between subaqueous deposits that are well sorted (matrix poor) or not (matrix rich). This contrasts with subaerial pyroclastic flow and fallout deposits, which occupy two distinct fields (Walker, 1971, 1983), although these values include fine clast data, allowing better characterization (Fig. 4). Matrix-poor, thin to thick, clast-supported, well sorted facies (MP-thin) have a much narrower range of standard deviation. Using median and sorting statistical parameters, the restriction of the grain size distribution to coarse clasts does not allow sufficiently accurate differentiation between the three types of subaqueous deposits of this study.

3.3 F-1 and D_{16}

The fine grain boundaries in volcaniclastic deposits are commonly destroyed during diagenesis, consolidation and/or sediment compaction (Jutzeler et al., 2012). The fine grains may be very abundant in volcaniclastic deposits, and are commonly used for classification. Here, we propose alternative statistical and volumetric measurements that avoid precise information on the fine grain size populations. These parameters can be used to compare data from both sieving and functional stereology.

F-1 represents the matrix ratio, corresponding to the volume ratio of <2 mm grains. Importantly, this ratio can be used as proxy for clast size sorting, because a large proportion of matrix in volcaniclastic rocks is a common indicator for poor sorting. On a cumulative curve, D_{16} corresponds to minimum clast diameter for 16 wt.% of the coarsest clasts. This statistical parameter was chosen as a balanced compromise: 1)

Most volcaniclastic deposits have at least 16% of clasts coarser than 2 mm, thus this parameter can be used widely. A bigger percentage (e.g. D_{50}) is not adequate, because it is likely to include large proportion of clasts <2 mm. 2) D_{16} is representative of a relatively large range of the coarse grain distribution. A lower statistical value (e.g. D_5, D_{10}) would only be representative of the coarse tail of the deposit, which is poorly constrained by both sieving and functional stereology data, due to clast outliers that are not part of modes and thus are non-representative of the global grain size distribution.

We plot F-1 against D_{16} for MR-thick, MR-thin and MP-thin (Fig. 5), and with sieving data from the KPT subaerial ignimbrite (Allen et al., 1999), which is used as proxy for subaerial pyroclastic flow deposits, although slightly finer grained than the average. The MR-thick, MP-thick and MP-thin data partly overlap, but show substantial differences in their range of F-1 and D_{16}, which can be attributed to their sorting and overall coarseness, respectively. MR-thick and MR-thin fully overlap with data from deposits D and E of KPT, indicating the coarse clasts have similar clast size in both types of deposits. MR-thick and MR-thin are relatively coarser grained than KPT data, which can be explained by the possible bias of field sieving where very coarse deposits cannot be easily sieved.

3.4. Hydraulic sorting ratio in pumiceous clastic rocks

The hydraulic sorting ratios for three main depositional processes are evaluated following equation (8), (12) and (13) for all samples of the three volcaniclastic facies in this study, as well as for basal dense-clast breccia of graded facies MP-thick and MR-thick.

3.4.1. Hydraulic sorting ratio in graded facies

The hydraulic sorting ratio of coarse components in most of the intervals in the graded bed at Bethells Beach in the Manukau Subgroup (Fig. 1f) is very close to 1 for relatively low vesicularity pumice (60 vol.% or 1,600 kg/m^3 wet density), reflecting very good hydraulic sorting in context of settling. However, the hydraulic sorting ratio by settling drops in the finer grained, poorly sorted uppermost part, probably due an increase of shear during last stage of deposition, as seen with a very good hydraulic sorting ratio for shear rolling. In contrast, the deposit at Pillow lava Bay is difficult to interpret, as its hydraulic sorting is not consistent in the stratigraphy, and settling and shear rolling are contenders as sedimentation processes. In addition, the dense clasts are mudstone, which may have a lower density than assumed.

The Dogashima Formation shows a relatively even trend of hydraulic sorting that approximates sorting by settling, considering pumice clasts are relatively high wet density (1,600 kg/m^3). However, this trend is cut by several intervals that show poor hydraulic sorting by settling, and where shear rolling is much more likely, reflecting abrupt changes in the conditions of sedimentation (e.g. units 2, 3e-top1, and 5a; Fig. 1f). In particular, bed 3e in the Dogashima 2 unit shows good hydraulic sorting by settling. This bed was originally interpreted as water-settled fallout from a submarine eruption umbrella plume by Cashman and Fiske (1991). Reappraisal of the Dogashima Formation using detailed stratigraphy and facies analysis (Jutzeler, 2012; Jutzeler et al., 2014a) led to the conclusion that this locally well-hydraulically sorted bed in Dogashima 2 was deposited from a seafloor-hugging density current that was locally inflated and turbulent due to interaction with a complex topography. Furthermore, gradational to sharp contacts of basal dense andesite breccia that contained hot clasts at deposition with overlying pumice breccia (units 2 to 4) implies deposition from an eruption-fed subaqueous volcaniclastic density current derived

from the collapse of a submarine magmatic-volatile-driven explosive eruption column (Jutzeler et al., 2014a). Such mechanism of deposition is matched by hydraulic sorting ratios showing that most of the sequence was deposited by settling (from a density current, considering stratigraphic relationships), with deposition of its basal dense andesite breccia (unit 2) by shear rolling. The low hydraulic sorting in units 3e-top1 and 5a, due to coarse dense clasts and fine pumice clasts (Fig. 1 e), is likely related to local current unsteadiness, or complex style of sedimentation.

In the Ohanapecosh Formation (Fig. 2), the hydraulic sorting ratios of MR-thick facies in the Ohanapecosh Formation are mostly less than 1, which indicates that the dense clasts are too coarse to be in hydraulic equivalence with pumice clasts. Apart from Cayuse 42 bed and top part of Chinook 61 bed, which shows good hydraulic sorting by settling, the poor hydraulic sorting of the MR-thick facies in the Ohanapecosh Formation suggests transport processes in which coarse clasts were not efficiently sorted by water during their settling, such as in high-concentration subaqueous volcaniclastic density currents that possibly had a weakly cohesive component (Jutzeler et al., 2014b). However, the good organization and grading of these beds precludes deposition from highly cohesive submarine debris flows. The low hydraulic sorting ratios may also partly be attributed to compaction of pumice clasts into fiamme (Jutzeler et al., 2012), artificially decreasing the grain size of the former pumice clasts. However, the hydraulic sorting ratio is too low to be exclusively caused by post-depositional compaction.

Several basal beds show low to very low hydraulic sorting ratios. At the base of the sequence in Dogashima (units 2, 3a), the lower section of fine pumice breccia (unit 5a, Dogashima), the basal dense-clast breccia of Cayuse 40 bed, Chinook 57 and 61, and Cougar Lake B3 (Figs 1, 2), dense clasts are much coarser than pumice clasts,

resulting in a very low hydraulic sorting by settling, but overall matching hydraulic sorting by shear rolling. These basal beds probably record deposition from a density current in which coarse dense clasts were transported by shear rolling at the base of the flow. Traction carpets can develop in the lower part of density currents (e.g. Sohn, 1997) and generate clast-supported basal sub-facies in which the coarsest and densest clasts are prominent due to depositional conditions.

3.4.2. Compiled hydraulic sorting ratios

The three types of hydraulic sorting ratio (settling, shear rolling, and collision rolling) from all waterlain deposits are compiled into Figure 6. This compilation allows inference on the major style of sedimentation in volcaniclastic settings. The hydraulic sorting ratios by settling show that a reasonably large amount of MR-thick, MP-thick and MP-thin deposits are reasonably hydraulically sorted with respect to settling (Fig. 6a-c), particularly where pumice density is relatively high (1,400-1,600 kg/m^3). In contrast, the basal dense-clast breccias are clearly not hydraulically sorted by settling from a density current, but show very good affinity with shear rolling (Fig. 6g). Hydraulic sorting by shear rolling also shows good affinity with our samples. This may indicate that some traction occurs during deposition of volcaniclastic density currents, however it is likely related to the small difference between both equations, resulting in shear rolling curves being relatively close to settling curves (Figs 1f and 2f). For collision rolling, our calculations show that whatever the pumice clast density, a very small amount of the studied facies were hydraulically sorted through this mechanism of deposition (Fig. 6d-f), strongly suggesting it is not represented in our samples.

4. Discussion

4.1. Applications of functional stereology to subaqueous volcaniclastic facies

The quantification of grain size distributions of volcaniclastic facies is greatly extended by using combined techniques of image analysis and functional stereology, developed in Jutzeler et al. (2012). Clast types and their relative volume can be determined by image analysis for any clastic deposit, unconsolidated or not, on the condition that the image shows a sufficiently even surface. Componentry and grain size grading of the coarse components can be assessed by sampling the same unit at various stratigraphic levels. From data extracted by image analysis, the grain size distribution of each clast type (e.g. pumice and dense clasts), as well as total clasts, can be determined by functional stereology.

The limitation of the technique to grain sizes coarser than 2 mm uniquely arises from the state of preservation of the samples. For instance, the grain size distribution of welded ignimbrites that contain well preserved matrix shards could ideally be calculated following the functional stereology approach, assuming the clast shapes can be simplified to a common geometry (Sahagian and Proussevitch, 1998).

The modes of V_i give an accurate description of the volumetric grain distribution of a clast population. Modes correspond to physical characteristics of aggregates, the most common grain sizes in a population, which are easier to visualize than the median. Extraction of modes from consolidated samples allows quantification of textural features such as grading (Figs 1d, 2d). Multiple modes in the grain size distribution of a clastic sample may record a complex history of fragmentation, transport and/or deposition (Wohletz et al., 1989).

4.2. A new, simple way to evaluate dominant underwater transport processes

The measurement of the proposed hydraulic sorting ratios gives new, valuable information on the mechanisms of transport and deposition of clastic deposits under

water. Our proposed three hydraulic sorting ratios, adapted to sedimentation under water from equations of Burgisser and Gardner (2006), provide tools to identify the best-fitted or dominant transport and sedimentation mechanisms. Deviations from the ideal hydraulic sorting ratios can be source of multiple causes, such as clasts having a wide range in vesicularity, source-controlled variations in the sediment supply (componentry, grain size), and complexities related to deposition mechanisms, including deposition of material from several levels in a stratified flow, interaction with topography, density stratification, and variations in fine particle concentration, momentarily modifying the flow rheology.

The use of the hydraulic sorting ratios on graded outcrops provide useful quantitative information to assess the modification of flow behavior through time at a single locality. For instance, the main sequence at Dogashima, and the beds Cayuse 40 and 42 and Chinook 57 in the Ohanapecosh Formation (Figs 1, 2) show graded facies MR-thick facies with basal dense-clast breccia emplaced by shear rolling, and overlain by pumiceous facies that show good hydraulic sorting under settling conditions; traction facies occur at the top (unit 4 at Dogashima, Cayuse 42). This sedimentation sequence matches classic examples (Postma et al., 1988; Talling et al., 2012) where initial deposition of coarse, dense clasts occurs from the basal dense-clast-rich part of a density current (that can develop into a traction carpet), and is progressively replaced by depositional settling from the main body of the density current at the boundary layer. Turbulence decreases in the uppermost part of the density current, where traction may develop.

4.3. Implications for transport and depositional processes

All studied water-lain pumiceous volcaniclastic deposits occupy a different field than subaerial pyroclastic flow deposits on the standard deviation versus median diagram

(Fig 4a). This effect is due to the much lower cut-off (+5 ϕ; $^{1}/_{32}$ mm) in sieved data used by Walker (1983) compared to the cut-off used in this study (-1 ϕ; 2 mm). Using the same cut-off (Fig. 4b), the coarse grained fraction (-6 to -1 ϕ; i.e. >2 mm) of the KPT sieving data overlap the field of matrix-rich, very thick, graded facies (MR-thick), and different types of deposits cannot be distinguished.

In the various subaqueous deposits examined, a better hydraulic equivalence by settling is found between the main modes of pumice and dense clasts if waterlogged pumice density spans 1,400–1,600 kg/m^3 than 1,200 kg/m^3. This relationship suggests (1) efficient waterlogging of the pumice clasts before their final deposition in water, which is likely considering the increasing confining pressure with increasing water depth during sedimentation; and (2) these submarine pumice were not exceedingly highly vesicular (60-75%; corresponding to 1,400–1,600 kg/m^3 waterlogged), which is reasonable. This inference is of critical importance in assessing the sources of pumice clasts deposited subaqueously.

Hot pumice clasts are efficiently waterlogged when quenched on contact with water (Whitham and Sparks, 1986; Allen et al., 2008), and can be deposited under water from subaqueous volcaniclastic density currents derived from subaerial pyroclastic flows that entered water (Whitham and Sparks, 1986; Freundt, 2003), or from subaqueous explosive eruptions (Allen and McPhie, 2009; Jutzeler et al., 2014a). Waterlogging of cold air-filled pumice clasts can require years (e.g. Whitham and Sparks, 1986; White et al., 2001; Jutzeler et al., 2014c).

4.4. Issues in using the median for grain size analyses

The median and standard deviation (Inman, 1952; Folk, 1980) are commonly used to compare the grain size distribution of different clast populations, and to discriminate the mode of emplacement of unconsolidated subaerial pyroclastic deposits (Moore,

1934; Murai, 1961; Walker, 1971; Walker and Croasdale, 1971; Walker, 1983, 1984). The median and standard deviation values were chosen for their simplicity in representing variations in grain size distributions and ease of calculations, both of which were important in the pre-computer era. However, the use of these parameters is commonly accompanied by two major statistical problems, rendering comparison of deposits unreliable. The two statistical problems are discussed below.

First, the median and standard deviation are meaningful only for monomodal and distributions (Folk, 1980). However, bi-modal and higher order poly-modal distributions are very common in pyroclastic deposits, and reflect poor sorting and diverse fragmentation, transport and/or depositional processes (e.g. Wohletz et al., 1989; Orsi et al., 1992). Both juvenile and non-juvenile clast populations can be responsible for secondary modes in the total grain size distribution (Walker, 1972, 1983; Wohletz et al., 1989; Carey and Houghton, 2010). Thus, the overall grain size median cannot identify discrete physical processes. Furthermore, some deposits may give the exact same values of median and standard deviation while these are evidently very different by distribution modes expressed in terms of mean values. We give two examples: (1) A monomodal distribution with a mode at 0 ϕ will have the same median as a bimodal distribution with same-magnitude modes at -3 and +3 ϕ; (2) A same sample will return different values of the median and standard deviation if the grain size distribution is calculated in the range -5 to +5 ϕ or over the range -5 to +3 ϕ. Second, modern techniques (e.g. laser diffraction; Evans et al., 2009) extend identification of the grain size to much finer clast diameters than sieving, but can be limited by maximum grain size it can detect. Comparison of the median and standard deviation of grain populations from datasets based on different cut-off grain sizes and/or on different techniques should not be attempted, because the actual range in

grain sizes and class size grading (bin sizes) are different in each given technique, instrument, or sieve set.

Therefore, we strongly argue that the use of the mode (i.e. the diameter of the most abundant grain size) to compare grain size distributions is more robust statistically. The main (primary) mode should broadly correspond to the visual (naked eye, hand lens) average grain size widely used during preliminary assessment of a deposit, and it makes sense to extend the use of such parameter to more in-depth studies. The main mode should be used to characterize the grain size of a deposit. All secondary modes (and eventual outsized coarse clasts) are crucially important to fully describe the grain size distribution of a sample, because these are likely caused by additional physical processes (i.e. fragmentation and/or sorting). F-1 and D_{16} are adequate to be used together with the modes to characterize volcaniclastic deposits.

4.5. Comparison of sieving and functional stereology datasets

Direct comparison of weight percent data from sieving and functional stereology is possible, but the thresholds of detection, especially for the fine-grained clasts, limit the scope of comparison with parameters such as median diameter and standard deviation. To compare sieving and functional stereology outputs in graphs of standard deviation versus median of Walker (1983) is difficult with data from this study, because particles <2 mm could not be separately identified from the clastic rocks. In addition, Walker's (1983) complete sieving dataset is not published, which precludes comparison of the coarse tails of his grain size distributions with our dataset. However, data from units D and E of the KPT ignimbrites (Allen et al., 1999), used as a proxy for pyroclastic flow deposits, match the field of matrix-rich, very thick, graded facies (MR-thick). Many of the samples analyzed by functional stereology and by sieving (e.g. Walker and Croasdale, 1971) contain two modes of coarse clasts (>2

mm) and it is likely that the matrix also includes one or more modes per sample. Consequently, because of the polymodal nature of the deposits, the median and standard deviation of all these data can only be compared qualitatively with unconsolidated subaerial equivalents.

We propose modes, F-1 and D_{16} as parameters to characterize volcaniclastic deposits, because detailed information on fine particles is not taken into account. These values can be extracted from both sieving and functional stereology data, are fully compatible, and do not need detailed textural data from the fine grain fractions.

5. Conclusions

We applied image analysis and functional stereology developed in Jutzeler et al. (2012) to clastic rocks of the Ohanapecosh Formation (Ancestral Cascades, Washington, USA), Dogashima Formation (Izu Peninsula, Japan), Manukau Subgroup (Northland, New Zealand) and the Sierra La Primavera caldera (Jalisco State, Mexico). This technique enables determination of textural features that conventional sieving methods are unable to retrieve on consolidated samples, such as clast and matrix volume, and grain size distribution. Matrix ratio, grain size modes, and several statistical parameters were extracted from the grain size distribution of (consolidated) pumiceous volcaniclastic rocks deposited in a subaqueous environment.

Modes, F-1 and D_{16} values allow characterization of the various subaqueous volcaniclastic facies, and these parameters can be directly compared with sieving data. We define three types of hydraulic sorting ratios, which quantifies how well a deposit is sorted hydraulically in three main types of transport and deposition, taking fluid density, clast size, and clast density into account. This ratio is especially relevant to

coarse clastic deposits containing different clast sizes and clast densities, such as pumice clasts versus dense clasts. The substantial amount of waterlain pumiceous volcaniclastic facies in this study (n=85) shows that clast with mixed densities were mainly deposited from settling processes, including from density currents or vertical settling. Minor influence from shear rolling cannot be excluded in many cases, and it is preponderant in dense clast basal breccias. Indeed, several density current deposits, such as at Dogashima (Japan) and in the Ohanapecosh Formation (USA), show a classic sedimentation sequence where initial deposition of dense clasts occurs at the base of the flow, possibly in a traction carpet, and is progressively replaced by deposition from settling from a subaqueous density current. Turbulence decreases in the uppermost part of the deposit, where traction may develop.

The relatively good hydraulic sorting by settling of pumice and dense clasts in most studied water-lain pumiceous deposits implies that the pumice clasts were cold and relatively dense (1,400–1,600 kg/m^3) at deposition, thus fully waterlogged, which was naturally achieved by contraction of any trapped gas in the clast porosity in response to increasing hydrostatic pressure during gravity-driven transport in water.

Figures

Figure 1

Image analysis and functional stereology on water-lain, graded, pumice-rich, volcaniclastic beds in the Dogashima Formation (Japan; MP-thick) and the Manukau Subgroup (New Zealand; MP-thin). a) Stratigraphic logs from field estimates. Stratigraphic logs show average grain size as black vertical line; outsized clasts reach out of the log; two vertical lines are used where dense and pumice clasts have distinct grain sizes; b) Clast, matrix and cement volume percent from image analysis; c) Volumetric componentry extracted from functional stereology data; d) Modal grain size distribution density per ϕ (G_i) from functional stereology. Outsized coarse clasts do not form modes, thus are not represented; e) Modal volume per ϕ (V_i) from functional stereology. Outsized coarse clasts do not form modes, thus are not represented; f) Three types of hydraulic sorting ratios at two end-member bulk wet densities for pumice clasts (gradient from plain to pale color for 1,200 kg/m^3 to 1,600 kg/m^3, respectively); g) Standard deviation (σ_ϕ) versus median (M_ϕ) values for samples from locations progressively up stratigraphy (arrows); analyzed grain size range is -12 to -1 ϕ (4 m to 2 mm). HSR, hydraulic sorting ratio.

Figure 2

Image analysis and functional stereology on water-lain, graded, pumice-rich volcaniclastic beds in the Ohanapecosh Formation (United States; MR-thick). a)

Stratigraphic logs from field estimates. Stratigraphic logs show average grain size as black vertical line; outsized clasts reach out of the log; two vertical lines are used where dense and pumice clasts have distinct grain sizes; b) Clast, matrix and cement volume percent from image analysis; c) Volumetric componentry extracted from functional stereology data; d) Modal grain size distribution density per ϕ (G_i) from functional stereology. Outsized coarse clasts do not form modes, thus are not represented; e) Modal volume per ϕ (V_i) from functional stereology. Outsized coarse clasts do not form modes, thus are not represented; f) Three types of hydraulic sorting ratios at two end-member bulk wet densities for pumice clasts (gradient from plain to pale color for 1,200 kg/m^3 to 1,600 kg/m^3, respectively); g) Standard deviation (σ_ϕ) versus median (M_ϕ) values for samples from locations progressively up stratigraphy (arrows); analyzed grain size range is -12 to -1 ϕ (4 m to 2 mm). HSR, hydraulic sorting ratio. See Fig. 1 for key.

Figure 3

Standard deviation (σ_ϕ) versus median (M_ϕ) of weight percent of water-lain samples of pumice-rich volcaniclastic facies MR-thick, MP-thick and MP-thin, from functional stereology of coarse clasts (-12 to -1 ϕ; 4 m to 2 mm). Samples from the Dogashima Formation, the Ohanapecosh Formation, the Manukau Subgroup and Sierra La Primavera caldera (Table 1). a) Pumice clast density are plotted as dry (700 kg/m^3, or 72% vesicles) for comparison with subaerial samples; b) Dense clasts with fixed density of 2,500 kg/m^3; c) Total clasts by combination of pumice and dense clasts datasets, taking the respective volume and vesicularities of pumice and dense clast classes into account; d) Contour of the total clasts datasets from (c).

Figure 4

Standard deviation (σ_ϕ) versus median (M_ϕ) from functional stereology (this study) and published sieving data. a) Coarse clast sizes (-12 to -1 ϕ; 4 m to 2 mm) from functional stereology of subaqueous volcaniclastic facies MR-thick, MP-thick and MP-thin (Fig. 3; Table 1) are compared with statistical percentage fields of 1% (short dash) and 4% (long dash) of total clast sizes by sieving at -5 to +5 ϕ (32 mm to 0.031 mm) of various types of unconsolidated subaerial pyroclastic deposits (Walker, 1983); b) Sieving and functional stereology data with different minimum cut offs in grain size. Sieving data of units D and E (subaerial ignimbrite) of the Kos Plateau Tuff (KPT; Allen et al., 1999) match the coarse, well-sorted part of Walker's (1983) field for subaerial pyroclastic flow deposits. When a minimum cut-off at -1 ϕ is applied, coarse-grained sieving data of units D and E of the KPT match fine-grained functional stereology data of subaqueous volcaniclastic deposits.

Figure 5

F-1 (i.e. matrix ratio) versus D_{16}, using full range of grain sizes (no cut-off). D_{16} corresponds to 16 wt.% of the coarsest clasts of each sample, and entirely consists of clasts coarser than 2 mm. a) Fields for MR-thick, MP-thick and MP-thin facies from functional stereology data partly overlap. b) Units D and E (subaerial ignimbrite) of the Kos Plateau Tuff (KPT; Allen et al., 1999) as proxy for subaerial pyroclastic flow deposits, largely overlap MR-thick and MP-thick facies.

Figure 6

Frequency histogram of the three hydraulic sorting ratios between pumice and dense clasts for MR-thick, MP-thick and MP-thin and basal dense-clast breccia for water-lain volcaniclastic facies. a-c, deposition by settling, varying the pumice density; d-f, deposition by collision rolling, varying the pumice density; g, deposition by shear

rolling. Pumice clast density varies as a function of vesicularity ratios. Densities

(kg/m^3) of pumice clasts, ρ_P; dense clasts, ρ_D; and seawater, ρ_w.

Tables

Table 1

Three comprehensive facies of volcaniclastic rocks analyzed by functional stereology,

from four waterlain successions: the Dogashima Formation (Japan), the Ohanapecosh

Formation (USA), the Manukau Subgroup (New Zealand) and Sierra La Primavera

caldera (Mexico) (Fiske, 1963; Clough et al., 1981; Cashman and Fiske, 1991; Allen

et al., 2007; Jutzeler, 2012; Jutzeler et al., 2014a; Jutzeler et al., 2014b).

References

Alfano, F., Bonadonna, C., Delmelle, P. and Costantini, L., 2011. Insights on tephra settling velocity from morphological observations. J. Volcanol. Geotherm. Res., 208, 86-98. doi:10.1016/j.jvolgeores.2011.09.013.

Allen, S.R. and Freundt, A., 2006. Resedimentation of cold pumiceous ignimbrite into water: Facies transformations simulated in flume experiments. Sedimentology, 53, 717-734. doi:10.1111/j.1365-3091.2006.00790.x.

Allen, S.R. and McPhie, J., 2009. Products of neptunian eruptions. Geology, 37, 639-642. doi:10.1130/G30007A.1.

Allen, S.R., Fiske, R.S. and Cashman, K.V., 2008. Quenching of steam-charged pumice; implications for submarine pyroclastic volcanism. Earth Planet. Sci. Lett., 274, 40-49. doi:10.1016/j.epsl.2008.06.050.

Allen, S.R., Hayward, B.W. and Mathews, E., 2007. A facies model for a submarine volcaniclastic apron: The Miocene Manukau Subgroup, New Zealand. Geol. Soc. Am. Bull., 119, 725-742. doi:10.1111/j.1365-3091.2006.00790.x.

Allen, S.R., Stadlbauer, E. and Keller, J., 1999. Stratigraphy of the Kos Plateau Tuff: Product of a major Quaternary explosive rhyolitic eruption in the eastern Aegean, Greece. Int. J. Earth Sci., 88, 132-156.

Blott, S.J. and Pye, K., 2001. Gradistat: A grain size distribution and statistics package for the analysis of unconsolidated sediments. Earth Surf. Processes Landforms, 26, 1237-1248.

Bonadonna, C. and Houghton, B.F., 2005. Total grain-size distribution and volume of tephra-fall deposits. Bull. Volcanol., 67, 441-456. doi:10.1007/s00445-004-0386-2.

Buller, A.T. and McManus, J., 1973. The quartile-deviation/median-diameter relationships of glacial deposits. Sediment. Geol., 10, 135-146.

Burgisser, A. and Gardner, J.E., 2006. Using hydraulic equivalences to discriminate transport processes of volcanic flows. Geology, 34, 157-160. doi:10.1130/G21942.1.

Carey, R.J. and Houghton, B.F., 2010. "Inheritance"; an influence on the particle size of pyroclastic deposits. Geology, 38, 347-350.

Carey, S., 1997. Influence of convective sedimentation on the formation of widespread tephra fall layers in the deep sea. Geology, 25, 839-842.

Carey, S.N., 1991. Transport and deposition of tephra by pyroclastic flows and surges. In: R.V. Fisher and G.A. Smith (Editors), Sedimentation in volcanic settings. SEPM, Tulsa; Special Publication, 45, pp. 39-57.

Cashman, K.V. and Fiske, R.S., 1991. Fallout of pyroclastic debris from submarine volcanic eruptions. Science, 253, 275-280. doi:10.1126/science.253.5017.275.

Clift, R., Grace, J.R. and Weber, M.E., 1978. Bubbles, drops, and particles. Dover Publications, Mineola, NY, USA, 381 pp.

Clough, B.J., Wright, J.V. and Walker, G.P.L., 1981. An unusual bed of giant pumice in Mexico. Nature, 289, 49-50. doi:10.1038/289049a0.

Crowe, C., Sommerfield, M. and Tsuji, Y., 1998. Multiphase flows with droplets and particles. CRC Press, Boca Ration, Flordia, 496 pp.

Dellino, P. et al., 2005. The analysis of the influence of pumice shape on its terminal velocity. 32. doi:10.1029/2005gl023954.

Dufek, J. and Bergantz, G.W., 2007. Dynamics and deposits generated by the Kos Plateau Tuff eruption: Controls of basal particle loss on pyroclastic flow transport. Geochem., Geophys., Geosyst., 8, Q12007. doi:10.1029/2007GC001741.

Evans, J.R., Huntoon, J.E., Rose, W.I., Varley, N.R. and Stevenson, J.A., 2009. Particle sizes of andesitic ash fallout from vertical eruptions and co-pyroclastic flow clouds, Volcán de Colima, Mexico. Geology, 37, 935-938. doi:10.1130/G30208A.1.

Fiske, R.S., 1963. Subaqueous pyroclastic flows in the Ohanapecosh Formation, Washington. Geol. Soc. Am. Bull., 74, 391-406. doi:10.1130/0016-7606(1963)74[391:SPFITO]2.0.CO;2

Folk, R.L., 1980. Petrology of sedimentary rocks. Hemphill Publ. Co., Austin, 184 pp.

Folk, R.L. and Ward, W.C., 1957. Brazos River bar [Texas]; a study in the significance of grain size parameters. J. Sediment. Petrol., 27, 3-26.

Freundt, A., 2003. Entrance of hot pyroclastic flows into the sea: Experimental observations. Bull. Volcanol., 65, 144-164.

Friedman, G.M., 1962. On sorting, sorting coefficients, and the lognormality of the grain-size distribution of sandstones. J. Geol., 70, 737-753.

Garzanti, E., Andò, S. and Vezzoli, G., 2009. Grain-size dependence of sediment composition and environmental bias in provenance studies. Earth Planet. Sci. Lett., 277, 422-432.

Glaister, R.P. and Nelson, H.W., 1974. Grain-size distributions, an aid in facies identification. Bull. Can. Pet. Geol., 22, 203-240.

Inman, D.L., 1952. Measures for describing the size distribution of sediments. J. Sediment. Petrol., 22, 125-145.

Jerram, D.A., Cheadle, M.J., Hunter, R.H. and Elliott, M.T., 1996. The spatial distribution of grains and crystals in rocks. Contrib. Mineral. Petrol., 125, 60-74.

Jutzeler, M., 2012. Characteristics and origin of subaqueous pumice-rich pyroclastic facies: Ohanapecosh Formation (USA) and Dogashima Formation (Japan). Ph.D. Thesis, University of Tasmania, Hobart, Australia, Hobart, Australia, 205 pp.

Jutzeler, M., McPhie, J. and Allen, S., 2014a. Submarine eruption-fed and resedimented pumice-rich facies: the Dogashima Formation (Izu Peninsula, Japan). Bull. Volcanol., 76, 1-29. doi:10.1007/s00445-014-0867-x.

Jutzeler, M., McPhie, J. and Allen, S.R., 2014b. Facies architecture of a continental, below-wave-base volcaniclastic basin: the Ohanapecosh Formation, Ancestral Cascades arc (Washington, USA). Geol. Soc. Am. Bull., 126, 352-376. doi:10.1130/B30763.1.

Jutzeler, M., Proussevitch, A.A. and Allen, S.R., 2012. Grain-size distribution of volcaniclastic rocks 1: A new technique based on functional stereology. J. Volcanol. Geotherm. Res., 239-240, 1-11. doi:10.1016/j.jvolgeores.2012.05.013.

Jutzeler, M. et al., 2014c. On the fate of pumice rafts formed during the 2012 Havre submarine eruption. Nat. Commun., 5, 3660. doi:10.1038/ncomms4660.

Kano, K., 1996. A Miocene coarse volcaniclastic mass-flow deposit in the Shimane Peninsula, SW Japan: Product of a deep submarine eruption? Bull. Volcanol., 58, 131-143. doi:10.1007/s004450050131.

Klug, C., Cashman, K. and Bacon, C., 2002. Structure and physical characteristics of pumice from the climactic eruption of Mount Mazama (Crater Lake), Oregon. Bull. Volcanol., 64, 486-501.

Komar, P.D. and Reimers, C.E., 1978. Grain shape effects on settling rates. J. Geol., 86, 193-209.

Komar, P.D., Baba, J. and Cui, B., 1984. Grain-size analyses of mica within sediments and the hydraulic equivalence of mica and quartz (Capistrano Formation, California). J. Sediment. Petrol., 54, 1379-1391.

Krumbein, W.C., 1936. Application of logarithmic moments to size-frequency distributions of sediments. J. Sediment. Petrol., 6, 35-47.

Kuno, H., Ishikawa, T., Taneda, S., Yagi, K. and Yamasaki, M., 1964. Sorting of pumice and lithic fragments as a key to eruptive and emplacement mechanism. Recent Progress of Natural Sciences in Japan = Nihon Shizen Kagaku Shuho, 35, 223-238.

Macedonio, G., Costa, A. and Folch, A., 2008. Ash fallout scenarios at Vesuvius: Numerical simulations and implications for hazard assessment. J. Volcanol. Geotherm. Res., 178, 366-377. doi:10.1016/j.jvolgeores.2008.08.014.

Mackaman-Lofland, C., Brand, B.D., Taddeucci, J. and Wohletz, K., 2014. Sequential fragmentation/transport theory, pyroclast size-density relationships, and the emplacement dynamics of pyroclastic density currents; a case study on the Mt. St. Helens (USA) 1980 eruption. J. Volcanol. Geotherm. Res., 275, 1-13. doi:10.1016/j.jvolgeores.2014.01.016.

Manville, V. and Wilson, C.J.N., 2004. Vertical density currents: A review of their potential role in the deposition and interpretation of deep-sea ash layers. J. Geol. Soc. (London, U. K.), 161, 947-958. doi:10.1144/0016-764903-067.

Manville, V., Segschneider, B. and White, J.D.L., 2002. Hydrodynamic behaviour of Taupo 1800a pumice: Implications for the sedimentology of remobilized pyroclasts. Sedimentology, 49, 955-976.

Manville, V., White, J.D.L., Houghton, B.F. and Wilson, C.J.N., 1998. The saturation behaviour of pumice and some sedimentological implications. Sediment. Geol., 119, 5-16. doi:10.1016/S0037-0738(98)00057-8.

McPhie, J., Doyle, M. and Allen, R., 1993. Volcanic Textures. ARC- Centre of Excellence in Ore Deposits University of Tasmania, Hobart, Australia, 198 pp.

Moore, B.N., 1934. Deposits of possible nuée ardente origin in the Crater Lake region, Oregon. J. Geol., 42, 358-375.

Murai, I., 1961. A study of the textural characteristics of pyroclastic flow deposits in Japan. Bulletin of the Earthquake Research Institute, 39, 133-248.

Orsi, G. et al., 1992. A comprehensive study of pumice formation and dispersal: the Cretaio Tephra of Ischia (Italy). J. Volcanol. Geotherm. Res., 53, 329-354.

Passega, R., 1964. Grain size representation by CM patterns as a geologic tool. J. Sediment. Petrol., 34, 830-847.

Postma, G., Nemec, W. and Kleinspehn, K.L., 1988. Large floating clasts in turbidites: a mechanism for their emplacement. Sediment. Geol., 58, 47-61.

Proussevitch, A.A., Sahagian, D.L. and Carlson, W.D., 2007a. Statistical analysis of bubble and crystal size distributions: Application to Colorado Plateau basalts. J. Volcanol. Geotherm. Res., 164, 112-126. doi:10.1016/j.jvolgeores.2007.04.006.

Proussevitch, A.A., Sahagian, D.L. and Tsentalovich, E.P., 2007b. Statistical analysis of bubble and crystal size distributions: Formulations and procedures. J. Volcanol. Geotherm. Res., 164, 95-111. doi:10.1016/j.jvolgeores.2007.04.007.

Reid, W.P., 1955. Distribution of sizes of spheres in a solid from a study of slices of the solid. J. Math. Phys., 34, 95-102.

Rubey, W.W., 1933. The size distribution of heavy minerals within a water-laid sandstone. J. Sediment. Petrol., 3, 3-29. doi:10.1306/D4268E37-2B26-11D7-8648000102C1865D.

Sahagian, D.L. and Proussevitch, A.A., 1998. 3D particle size distributions from 2D observations: Stereology for natural applications. J. Volcanol. Geotherm. Res., 84, 173-196. doi:10.1016/S0377-0273(98)00043-2.

Sallenger, A.H., 1979. Inverse grading and hydraulic equivalence in grain flow deposits. J. Sediment. Petrol., 49, 553-562.

Sengupta, S., Ghosh, J.K. and Mazumder, B.S., 1991. Experimental-theoretical approach to interpretation of grain size frequency distributions. In: J.P.M. Syvitski (Editor), Principles, methods, and application of particle size analysis. Cambridge Univ. Press, New York, pp. 264-279.

Shea, T. et al., 2010. Textural studies of vesicles in volcanic rocks: An integrated methodology. J. Volcanol. Geotherm. Res., 190, 271-289. doi:10.1016/j.jvolgeores.2009.12.003.

Sohn, Y.K., 1997. On traction-carpet sedimentation. J. Sediment. Res., 67, 502-509.

Sparks, R.S.J., 1976. Grain-size variations in ignimbrites and implications for transport of pyroclastic flows. Sedimentology, 23, 147-188.

Sparks, R.S.J., Self, S. and Walker, G.P.L., 1973. Products of ignimbrite eruptions. Geology, 1, 115-118.

Talling, P.J., Masson, D.G., Sumner, E.J. and Malgesini, G., 2012. Subaqueous sediment density flows: Depositional processes and deposit types. Sedimentology, 59, 1937-2003. doi:10.1111/j.1365-3091.2012.01353.x.

Tamura, Y., Koyama, M. and Fiske, R.S., 1991. Paleomagnetic evidence for hot pyroclastic debris flow in the shallow submarine Shirahama Group (Upper Miocene-Pliocene), Japan. J. Geophys. Res., 96, 21779-21787. doi:10.1029/91JB02258.

Visher, G.S., 1969. Grain size distributions and depositional processes. J. Sediment. Petrol., 39, 1074-1106.

Volentik, A.C.M., Bonadonna, C., Connor, C.B., Connor, L.J. and Rosi, M., 2010. Modeling tephra dispersal in absence of wind: Insights from the climactic phase of the 2450BP Plinian eruption of Pululagua volcano (Ecuador). J. Volcanol. Geotherm. Res., 193, 117-136. doi:10.1016/j.jvolgeores.2010.03.011.

Walker, G.P.L., 1971. Grain-size characteristics of pyroclastic deposits. J. Geol., 79, 696-714.

Walker, G.P.L., 1972. Crystal concentration in ignimbrites. Contrib. Mineral. Petrol., 36, 135-145.

Walker, G.P.L., 1983. Ignimbrite types and ignimbrite problems. J. Volcanol. Geotherm. Res., 17, 65-88.

Walker, G.P.L., 1984. Characteristics of dune-bedded pyroclastic surge bedsets. J. Volcanol. Geotherm. Res., 20, 281-296.

Walker, G.P.L. and Croasdale, R., 1971. Two Plinian-type eruptions in the Azores. J. Geol. Soc. (London, U. K.), 127, 17-55.

Wentworth, C.K., 1922. A scale of grade and class terms for clastic sediments. J. Geol., 30, 377-392.

White, J.D.L., 2000. Subaqueous eruption-fed density currents and their deposits. Precambrian Res., 101, 87-109. doi:10.1016/S0301-9268(99)00096-0.

White, J.D.L. and Houghton, B.F., 2006. Primary volcaniclastic rocks. Geology, 34, 677-680. doi:10.1130/G22346.1.

White, J.D.L. et al., 2001. Settling and deposition of AD 181 Taupo pumice in lacustrine and associated environments. In: J.D.L. White and N.R. Riggs (Editors), Volcaniclastic sedimentation in lacustrine settings. Blackwell Science, Oxford, England, pp. 141-150.

Whitham, A.G. and Sparks, R.S.J., 1986. Pumice. Bull. Volcanol., 48, 209-223. doi:10.1007/BF01087675.

Wiesner, M.G., Yubo, W. and Lianfu, Z., 1995. Fallout of volcanic ash to the deep South China Sea induced by the 1991 eruption of Mount Pinatubo (Philippines). Geology, 23, 885-888.

Wilson, C.J.N. and Walker, G.P.L., 1985. The Taupo eruption, New Zealand. I. General aspects. Philos. Trans. R. Soc., A, 314, 199-228.

Wohletz, K.H., Sheridan, M.F. and Brown, W.K., 1989. Particle size distributions and the sequential fragmentation/transport theory applied to volcanic ash. J. Geophys. Res., 94, 15703-15721. doi:10.1029/JB094iB11p15703.
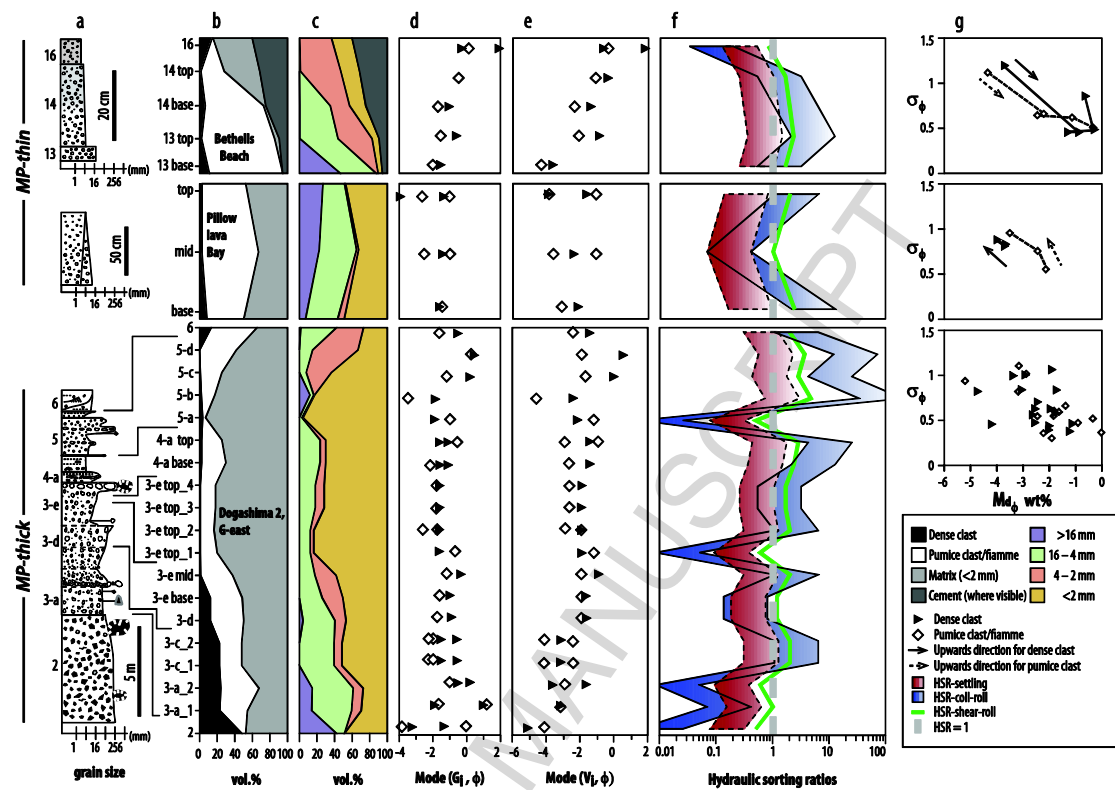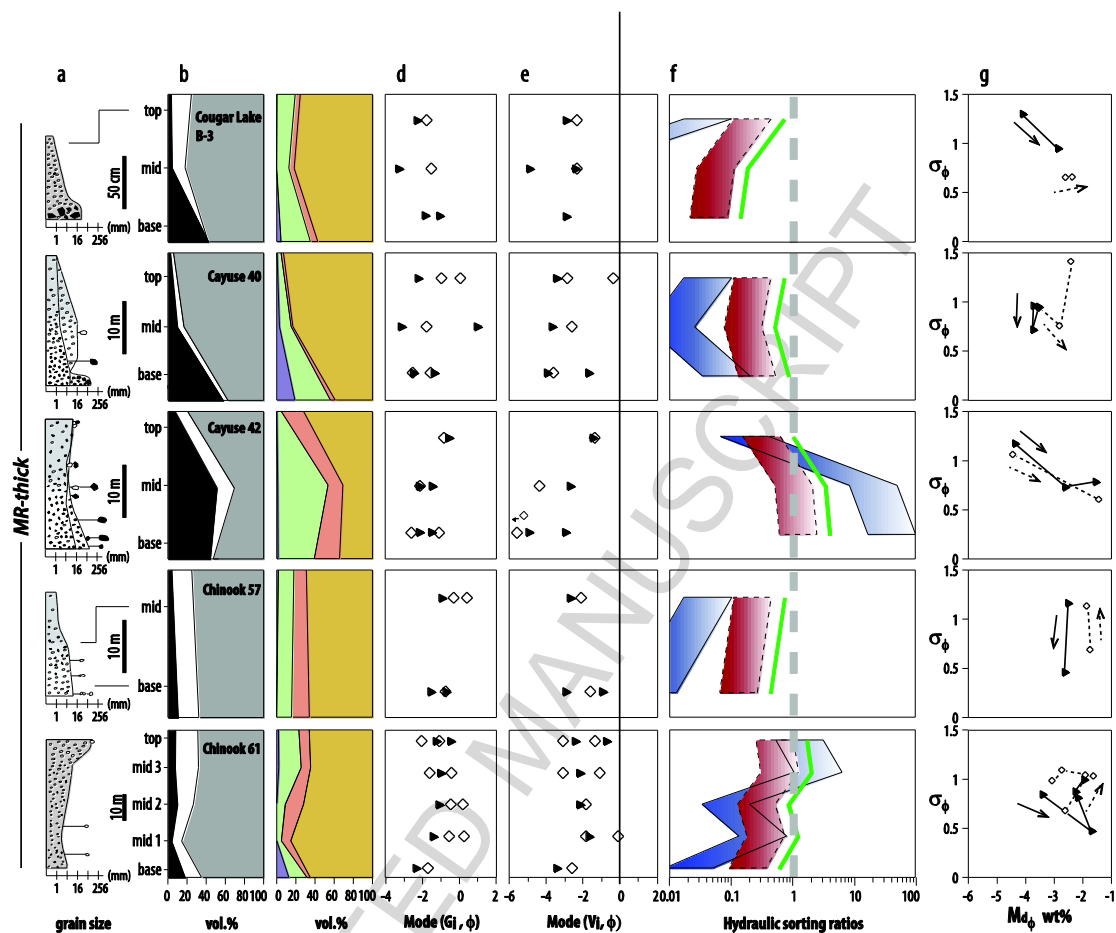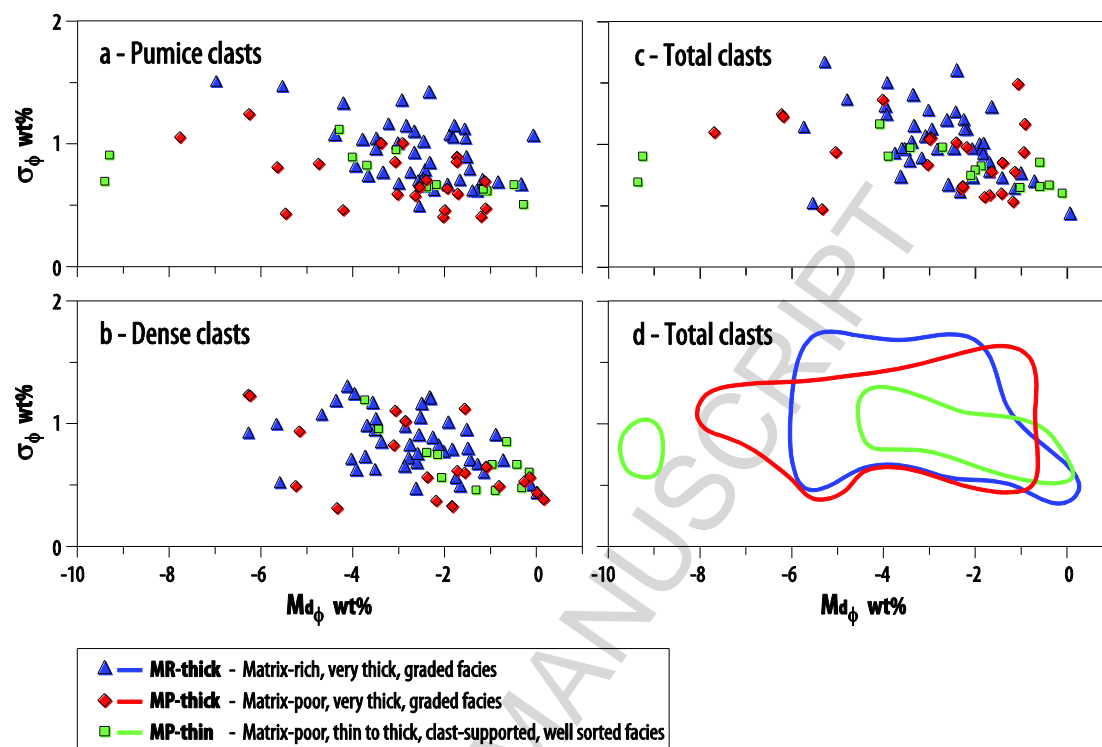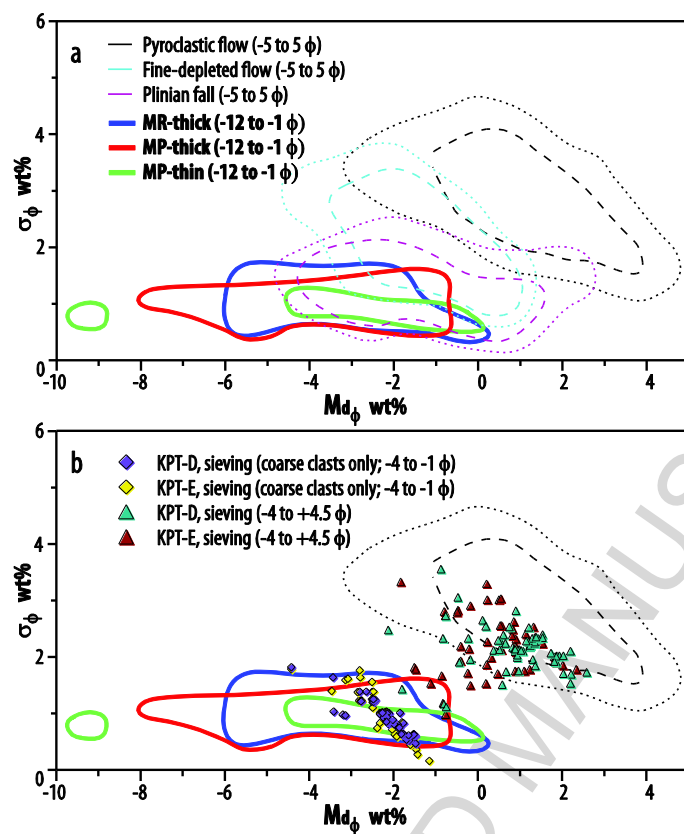
Figure 1

Figure 2

Figure 3

Figure 4

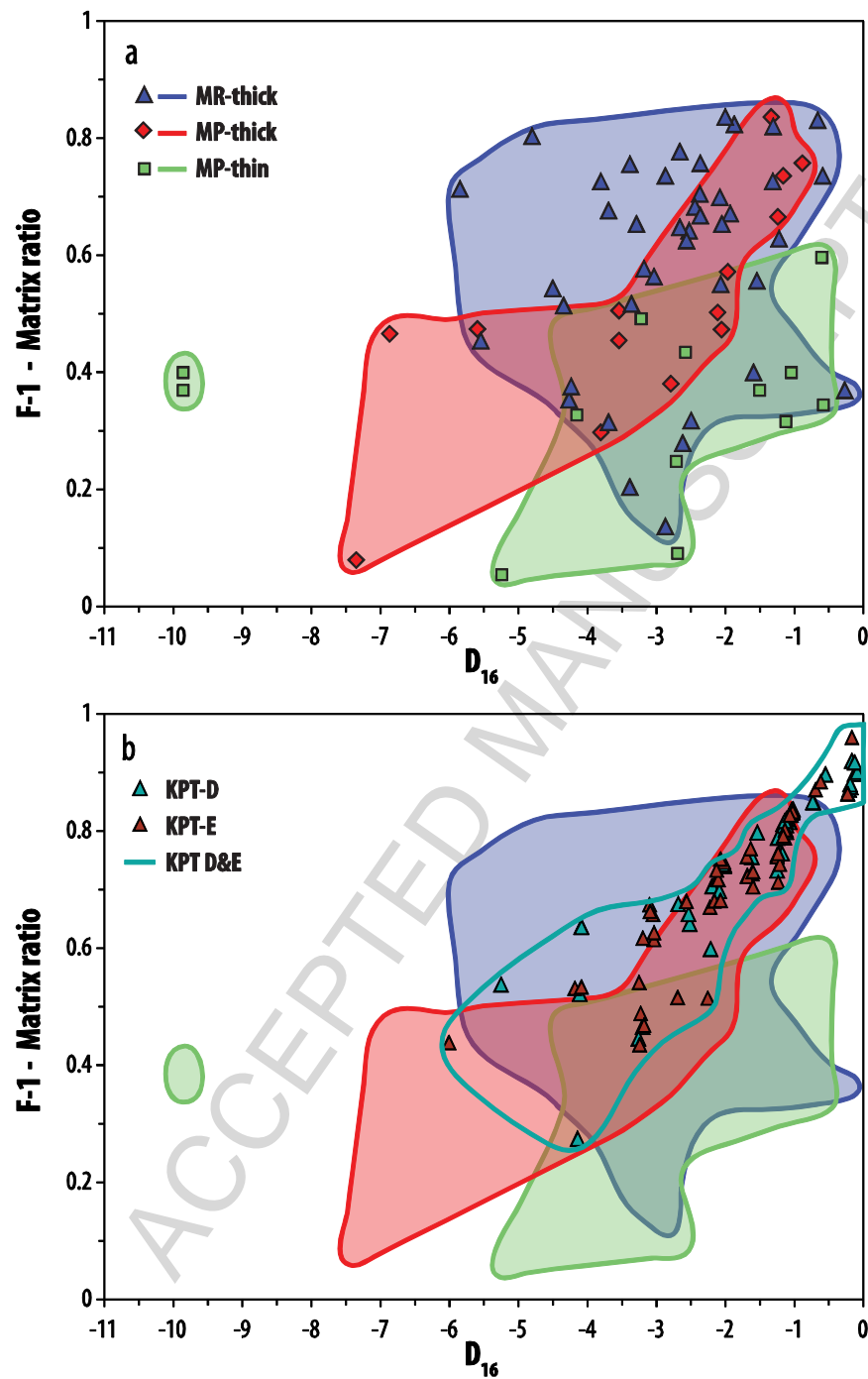**Figure 5**

Figure 6

Table 1

Facies name	Number of samples	Facies characteristics	Interpreted transport	Formation/ Sub-Group
MR-thick	46	Matrix-rich, very thick, graded facies	Subaqueous volcaniclastic density current	Ohanapecosh, Dogashima, Manukau
MP-thick	25	Matrix-poor, very thick, graded facies	Subaqueous volcaniclastic density current	Dogashima 1 and 2, Ohanapecosh
MP-thin	14	Matrix-poor, thin to thick, clast-supported, well sorted facies	Subaqueous vertical settling	Manukau, Ohanapecosh, Primavera caldera

Highlights:

Functional stereology is efficient to interpret sedimentation mechanisms

Simple hydraulic sorting ratios allow inference on styles of deposition

Transport and deposition mechanisms can be evaluated from pumiceous rocks

Modes are more adequate than median to characterize sediment grain size